International Journal of Climatology

Climate change projections for olive yields in the Mediterranean Basin

Journal:	*International Journal of Climatology*
Manuscript ID	JOC-19-0237.R1
Wiley - Manuscript type:	Research Article
Date Submitted by the Author:	03-Jun-2019
Complete List of Authors:	Fraga, Helder; Universidade de Trás-os-Montes e Alto Douro, Centre for the Research and Technology of Agro-Environmental and Biological Sciences Pinto, Joaquim; Karlsruher Institut fur Technologie Institut fur Meteorologie und Klimaforschung, Institute of Meteorology and Climate Research Viola, Francesco ; Università degli Studi di Cagliari, Department of Civil Environmental and Architectural Engineering Santos, João; Universidade de Trás-os-Montes e Alto Douro, Centre for the Research and Technology of Agro-Environmental and Biological Sciences
Keywords:	Olive yields, climate change, Euro-Cordex, Representative Concentration Pathways, Europe, Climate < 2. Scale, Land-atmosphere < 4. Geophysical sphere, Agrometeorology < 6. Application/context
Country Keywords:	Spain, Portugal, France, Italy, Greece

Climate change projections for olive yields in the Mediterranean Basin

Helder Fraga[a,b,1]; Joaquim G. Pinto[b]; Francesco Viola[c]; João A. Santos[a]

[a]*Centre for the Research and Technology of Agro-Environmental and Biological Sciences (CITAB), Universidade de Trás-os-Montes e Alto Douro (UTAD), Vila Real, Portugal*

[b]*Institute for Meteorology and Climate Research (IMK-TRO), Karlsruhe Institute of Technology (KIT), Karlsruhe, Germany*

[c]*Department of Civil Environmental and Architectural Engineering, Università degli Studi di Cagliari, Cagliari, Italy*

Short title: European olive trees under climate change scenarios

Revision 1 submitted to:

International Journal of Climatology

[1]*The corresponding author*: Helder Fraga, E-mail: hfraga@utad.pt, Tel: +351259350000

Abstract

The olive tree is one of the most important crops in the Mediterranean basin. Given the strong climatic influence on olive trees, it becomes imperative to assess climate change impacts on this crop. Herein, these impacts were innovatively assessed, based on an ensemble of state-of-the-art climate models, future scenarios and dynamic crop models. The recent-past (1989–2005) and future (2041–2070, RCP4.5 and RCP8.5) olive growing season length (GSL), yield, growing season temperature (GST) and precipitation (GSP), potential (ETP) and actual (ETA) evapotranspiration, water demand (WD) and water productivity (WP), were assessed over southern Europe. Crop models were fed with an ensemble of EURO-CORDEX regional climate model data, along with soil and terrain data. For the recent-past, important differences between western and eastern olive growing areas are found. GSL presents a strong latitudinal gradient, with higher/lower values at lower/higher latitudes. Yields are lower in inner south Iberia and higher in Italy and Greece, which is corroborated by historical data. Southern Iberia shows higher GST and lower GSP, which contributes to a higher ETP, lower ETA and consequently stronger WD. Regarding WP, the recent-past values shows similar ranges across Europe. Future projections point to a general increase in GSL along with an increase in GST up to 3ºC. GSP is projected to decrease in Western Europe, leading to enhanced WD and consequently a yield decrease (down to -45%). Over eastern European, GSP is projected to slightly increase, leading to lower WD and to a small yield increase (up to +15%). WP will remain mostly unchanged. We conclude that climate change may negatively impact the viability of olive orchards in southern Iberia and some parts of Italy. Thus, adequate and timely planning of suitable adaptation measures are needed to ensure the sustainability of the olive sector.

Keywords: Olive yields; Europe; climate change; Euro-Cordex; Representative Concentration Pathways

1. Introduction

The olive tree (*Olea europaea* L.) is one of the oldest permanent crops grown in the Mediterranean basin (Vossen, 2007). This perennial and evergreen tree has a strong socio-economic importance for many southern European countries, which encompass 80% of the worldwide olive tree area (EC, 2012) **(Fig. 1)** and produce roughly 95% of the world olive oil supply. Olive production is concentrated in the Mediterranean-type climatic regions of southern Europe, particularly Spain (53%), Italy (24%), Greece (15%) and Portugal (7%) , amongst others (EC, 2012). Since olive oil is traditionally exported worldwide, this crop became one of the foundations for the economic development in agrarian regions in these countries (IOC, 2018).

Traditional olive orchards in the Mediterranean basin present very specific climatic requirements, required to attain high production levels and quality attributes (Vossen, 2007). This crop is considered one of the most suitable and best adapted species to the Mediterranean-type climate (Moriondo *et al.*, 2015, Orlandi *et al.*, 2012). In fact, the location of olive orchards in this specific region of the globe is primarily explained by climatic factors. While temperatures below -5 °C damage olive branches and significantly limit its poleward expansion, the lack of cold temperatures - necessary to ensure a proper flowering - limit its equatorward distribution (Moriondo *et al.*, 2015). Olives are also very drought-tolerant, as the lower limit for annual precipitation is around 350 mm (Ponti *et al.*, 2014). As such, the olive tree is usually grown under rain-fed conditions (Gomez-Rico *et al.*, 2007). All these aspects make the olive tree particular suitable for the Mediterranean-type climate (Moriondo *et al.*, 2015), which is characterized by warm dry summers and rainy winters. However, soil fertility and soil water holding capacity may also play an important role for olive tree development.

The Mediterranean basin is considered a climate change “hotspot” (Giorgi, 2006), since future projections point to considerable warming trends and an increase of consecutive dry days for this area (IPCC, 2012), leading to an overall increase in aridity. In this context, climate change may become particularly challenging for olive growers (Moriondo *et al.*, 2015). Recent studies applied to olive trees have shown that this crop can be strongly affected by climate change (Orlandi *et al.*, 2005, Osborne *et al.*, 2000, Ponti *et al.*, 2014) particularly under the Mediterranean type-climates (Galán *et al.*, 2005, Orlandi *et al.*, 2010). For instance, rising temperatures may have strong impacts on this crop, advancing phenological timings, particularly flowering (Avolio *et al.*, 2012, Galán *et al.*, 2005, Orlandi *et al.*, 2010, Osborne *et al.*, 2001). Fraga *et al.* (2019) points to a strong change in thermal conditions for olive trees in Europe until the end of this century. Other studies suggest a gradual poleward shift of current olive cultivation areas in the upcoming decades, due to increased suitability in higher latitudes (Moriondo *et al.*, 2013, Tanasijevic *et al.*, 2014). In spite of these efforts, there is a strong need to improve our knowledge on how future climate may affect olive yields. As an example, Ponti *et al.* (2014), using a single future climate scenario (A1B) and a single climate model, projected high economic losses for small olive farms in Italy and Greece. Still, there is a need to perform comprehensive assessments based on multi-model multi-scenario ensembles in order to derive robust yield estimates and provide a measure of its uncertainly under future climate conditions (Deser *et al.*, 2012).

Crop models are gradually becoming reliable tools to support decision making within the agrarian sector (Challinor & Wheeler, 2008, Paz *et al.*, 2007, Semenov & Doblas-Reyes, 2007). Crop models can be either statistical/empirical or dynamical/process-based in their nature. While statistical models try to establish relationships between e.g. historical yields and climate data, dynamic models inherently simulate plant growth and development by integrating varietal information, soil characteristics, weather data and management practices

(Moriondo *et al.*, 2015). Despite being applied to a large array of crops worldwide (e.g. wheat, maize, rice), crop models are still not widely used for olive trees. Still, some statistical models do exist, which relate growing season temperatures, particularly during spring, with phenological timings and yields (Aguilera *et al.*, 2015, Garcia-Mozo *et al.*, 2008, Moriondo *et al.*, 2001, Orlandi *et al.*, 2012, Oteros *et al.*, 2014, Quiroga & Iglesias, 2009). Regarding dynamical models, some models are devoted to access phenological stages of olive tree growth and development (Cesaraccio *et al.*, 2004, De Melo-Abreu *et al.*, 2004, Moriondo *et al.*, 2019), while others are aimed to predict biomass growth (Maselli *et al.*, 2012, Villaobos *et al.*, 2006, Viola *et al.*, 2012). Given their large complexity, dynamic models usually tend to be preferable to statistical approaches, as they simulate plant physiology and its relationships with the surrounding environment. Furthermore, dynamical models are continuously updated with new scientific knowledge. These dynamical crop models can thus lead to reliable and robust future projections of yield, growing season length and stress indicators over a wide region when coupled with high resolution climate model simulations, consistent soil and plant data.

The present study aims to develop and analyse climate change projections for the olive sector in the Mediterranean basin. As such, the objectives of this study are three-fold: 1) to couple a dynamic crop model with high resolution climatic simulations for current climates and for future climate change scenarios; 2) to develop climate change projections for olive yield, growing season and stress conditions in the most important olive producing regions in the Mediterranean basin; and 3) to discuss the impacts of climate change on the European olive sector and possible adaptation measures.

2. Material and Methods

2.1 Study area

In order to assess the distribution of olive orchards in southern Europe, the CORINE Land Cover (CLC, v18.5.1), was used. This dataset is derived from satellite imagery and mapping of land inventories, providing land usage classes over most of Europe. The olive orchard polygons were extracted for subsequent processing. All computations in the present study were performed only inside the current olive orchard land cover delimitations **(cf. Fig. 1)**. A more detailed analysis was also performed on some of the European top olive producing regions, such as (from west-to-east): (1) Alentejo in Portugal; (2) Andalucía, (3) Extremadura and (4) Castilla la Mancha in Spain; (5) Sardegna , (6) Sicily and (7) Puglia in Italy; and (8) Peloponnese in Greece **(Fig. 1)**. For this purpose, the Nomenclature of Territorial Units for Statistics - level 2 (NUTS-2) classification was used to delineate the regions. Other olive growing regions were not considered due to limitations in the various datasets.

2.2 Crop Model description

To model olive yields, the dynamic crop model developed by Viola *et al.* (2012) was used (henceforth yield-model). This is a water-driven crop model that "links olive yield to climate and soil moisture dynamics using an ecohydrological approach" (Viola *et al.*, 2012). In a recent review of current dynamic crop models applied to olive trees, Moriondo *et al.* (2015) described this model underlining the keys aspects. The leaf area index influences the light interception model. Dry matter formation is governed by the photosynthesis and respiration models. The photosynthesis model takes the atmospheric CO_2 levels into account, while the transpiration model follows the implementation by Villalobos *et al.* (2000). The conversion of biomass into final yield is influenced by water stress. Indeed, dry matter partitioning and potential biomass are limited by water availability in the soil, which in turn is governed by rainfall inputs and vegetation withdrawal. The latter, without soil moisture limitations is modelled with the Penman-Monteith Big Leaf model, which explicitly takes into account the effect of CO_2 concentration in the photosynthesis model. All simulations herein were performed continuously without any re-initialization in order examine certain carry-over effects on the final yields, such as the stress duration and intensity. Other effects, such as alternate bearing or changes in partition coefficients, are not considered. For additional information regarding this model please see Viola *et al.* (2012).

This model runs on a daily time-step, simulating crop development from the start until the end of the growing season and requires a large number of parameters describing local conditions, such as soil profile characteristics (e.g. soil hydraulic conductivity and soil porosity), technical parameters (e.g. leaf area index, crop ground cover fraction, growing season start and end) and weather daily data (precipitation, maximum and minimum temperatures, radiation, relative humidity, wind speed and CO_2). All these parameters were used as model input and are described in the subsequent sections.

In order to access the olive tree growing season (required by the yield-model), the model developed by Orlandi *et al.* (2013) was used (henceforth season-model). This is a very simple regional model that provides the annual start and end of the vegetative cycle (leaf development start to fruit coloration) based on a bioclimatic "growing season index" of olive trees (Orlandi *et al.*, 2013). This index is derived only from climatic data and was properly validated for the Mediterranean olive tree areas (Orlandi *et al.*, 2013). Both models (season-model and yield-model) were therefore coupled.

2.3 Climate data

The required daily meteorological variables by the two crop models are: maximum air temperature (ºC), minimum air temperature (ºC), solar radiation ($W.m^{-2}$), total precipitation (Prec; mm), wind speed ($m.s^{-1}$), relative humidity (%) and CO_2 levels (ppmv). All these variables were obtained from EURO-CORDEX datasets (Jacob *et al.*, 2014), an ensemble of regional climate model simulations at a ~12.5 km spatial resolution covering the southern European sector. For the recent-past period (1989-2005), we consider four regional climate models (RCM, **Table 1**) driven with ERA-Interim reanalysis (Dee *et al.*, 2011) as boundary conditions (EURO-CORDEX evaluation runs). 1989-2005 was considered since it is the overlapping time period available for all the climate models for the recent-past. This dataset represents real-world climate over the selected period. Within the EURO-CORDEX project framework, the RCMs were also forced by four global climate models (GCM, **Table 1**) for 1989-2005 (historical runs) and for 2041-2070 following the RCP4.5 and RCP8.5 scenarios. In RCP4.5, CO_2 emissions are projected to increase until the mid-21st century, decreasing afterwards (IPCC, 2012). In contrast, in RCP8.5, the CO_2 emissions continue to rise until the end of the 21st century. The CO_2 values correspond to 497 and 598 ppm (on average for 2041-2070), for RCP4.5 and RCP8.5, respectively.

The daily variables produced by the RCM-GCM chains were first bias-corrected for 1989-2005 using the evaluation runs as a reference and following the "Empirical Quantile Mapping" methodology (Cofiño *et al.*, 2017). This correction was subsequently applied to the future period (2041-2070), thus obtaining future bias corrected data. This methodology was previously carried out by several studies, e.g. Fraga *et al.* (2019). Lastly, the bias-corrected gridded climatic variables were then used as input for the crop models.

2.3 Soil and plant data

Each grid-box in the climatic datasets was treated as an independent site in the crop models. Other required variables were defined based on the location of these grid-boxes, such as soil and terrain characteristics. Soil data was obtained from the Harmonized World Soil Database (HWSD; FAO/IIASA/ISRIC/ISSCAS/JRC, 2012). Soil properties from the HWSD were extracted based on the predominant soil type inside each grid-box (**Table 2**). Some soil parameters were estimated using the pedotransfer functions also described in **Table 2**. For a large-scale comprehensive modelling approach throughout southern Europe, some assumptions were made concerning grown varieties and cultural practices. Hence, plant data was set as standard for all grid-boxes, following Viola *et al.* (2012): leaf area index (1.4 $m^2.m^{-2}$); root depth (100 cm) and canopy cover fraction (0.4).

2.4 Modelling outputs

The current study focuses only on the area currently covered by olive trees, which is mostly confined to some regions in southern Europe (**Fig. 1**). Therefore, both the yield-model and the season-model were run for all grid-boxes within these delimitations, separately for each climate model and each year. While crop model runs were performed for each climate model separately, the outcomes of these runs were averaged for all climate models (ensemble means) in order to obtain more robust future projections. The annual outputs collected for the recent-past and for each future scenario were: growing season start (GSS, calendar day), growing season end (GSE, calendar day), growing season length (GSL = GSE – GSS in number of days), yield ($kg.ha^{-1}$), growing season potential evapotranspiration (ETP, mm) and growing season actual evapotranspiration (ETA, mm). Other two important water use related metrics that greatly influence olive yields were also computed: the growing season water deficit (WD, mm), which corresponds to ETP minus ETA (Moriondo *et al.*, 2013), and the growing season water productivity (WP; $kg.ha^{-1}.mm$), i.e. yield divided by ETA (Perry, 2011). Additionally, the growing season mean temperature (GST) and growing season precipitation (GSP) were also computed. Lastly, the annual outcomes were averaged for each time period (1989–2005 and 2041–2070) and mapped throughout the southern European sector. Statistically significant differences between the future and the recent-past were also assessed and mapped at a 99% confidence level, using the two-sample *Student's t-test*.

Both crop models have been previously validated. Regarding the season-model, Orlandi *et al.* (2013) showed a strong relationship between GSS (GSE) and leaf development start (fruit coloration) (root-mean-squared errors of 1.73 or 0.58 days, respectively), over olive regions in Italy, Spain and Tunisia. For the yield-model, Viola *et al.* (2012) successfully validated the model for olive orchard site in Italy. Nonetheless, we perform a comparison between the modelled yields and the national olive yield statistics from the Food and Agriculture Organization of the United Nations (FAO; http://faostat.fao.org/) (**Fig. 1**). Additionally, data from the EUROSTAT regional dataset was also collected, though a comparison was not possible due to important data gaps found in this dataset, both spatially and temporally. This data corresponds to a large number of varieties (mixed varieties) and years, which does not exactly correspond to the historical time period used herein. Still, this validation effort is useful to assess whether the yield-model is able to capture the magnitude and heterogeneity of yield values in Europe.

3. Results

3.1 Recent-past assessment

The GSL for the recent-past, computed by the season-model, is shown in **Figure 2a**. Overall, the olive tree GSL ranges from 200 days in the cooler regions of northern Italy and southern France, to 220-230 days in Iberia, Greece, Albania and southern Italy, reaching a maximum of 250 in southern Iberia. A latitudinal gradient is clearly visible in the GSL patterns, where the northern (southern) regions show lower (higher) number of days in the growing season. This indicates that the olive tree growing season is typically longer for western Europe.

Regarding yields (**Fig. 2b**), the simulations show higher values in Italy and some areas of Albania and Greece (>2000 kg/ha) and lower values in southeastern Iberia (~1000 kg/ha). The magnitude of the simulated values is in agreement with the regional statistical dataset (**Fig. 1**), and the model is also able to resolve longitudinal yield differences that are visible in the statistical dataset, e.g., the higher yields in Italy and Greece compared to Iberia. Still, some discrepancies are found between the simulated and the statistical dataset. Overall, the model simulates slightly higher values than those found in the statistical dataset (**Fig. 1**).

GST for the recent-past (**Fig. 2c**) ranges from 12 ºC at higher elevation and cooler areas to 24 ºC in inner Iberia and some regions in southeastern Italy and in Greece. The cooler regions include northern Portugal, northern Italy and in the (southern) French olive growing regions. Regarding GSP (**Fig. 2d**), the map presents very homogeneous patterns, with most of the olive productive regions showing values from 200 to 300 mm, with the exception of areas in central/northern Italy and in southern France, where precipitation amounts exceed 300 mm.

Water availability is an important factor affecting plant physiological activity, particularly in arid and semi-arid regions, such as in the Mediterranean (Aissaoui *et al.*, 2016). For the recent-past, the growing season ETP (**Fig. 2e**) shows higher values in southern Iberia, from ~1000 mm to around 600 mm in northern Italy. However, most of the olive orchard areas in southern Europe present ETP values from 800 to 1000 mm. In effect, ETP patterns are highly correlated with the GST (r = +0.8), since temperature strongly influences this metric.

Regarding ETA (**Fig. 2f**), a metric that takes into account the amount of water that is effectively used by the plant, this metric shows heterogeneous values across Europe. The ETA ranges from 200 mm, in southeastern Iberia, to 500 mm, in some regions in inner Italy and in costal Croatia and Albania. Nonetheless, most of the olive orchards in Europe have ETA values from 300 to 400 mm.

Given the difference between ETP and ETA, higher water deficits are found for the current olive tree area (**Fig. 2g**), suggesting high water scarcity. During the growing season (**Fig. 2g**), WD reaches values of ~750 mm in southern Iberia (in some areas even 900 mm), in Sicily and in Sardegna. The lowest WD values are found in northern Italy, southern France and some coastal areas of the Adriatic. Most of southern European olive orchards are thus growing under relatively high water deficits. Regarding WP, this index displays relatively homogeneous values throughout the olive growing areas (**Fig. 2h**). Values higher than 5 $kg.ha^{-1}.mm^{-1}$ are widespread, with the exception of some areas in inner Iberia, with values of ca. 4 $kg.ha^{-1}.mm^{-1}$.

3.2 Future climate projections

The bias corrected projections from EURO-CORDEX (section 2.2.) are now considered to estimate the impact of climate change to the olive orchards. Results point to an extension in the length of the growing season under RCP4.5 (**Fig. 3a**) and RCP8.5 (**Fig. 4a**). In effect, there is a clear increase of the GSL throughout Europe by up to 10 days, which hints at higher temperatures throughout the growing season. The increase of the GSL ranges from 2 to 10 days, with the strongest increase occurring in south-eastern Spain and for RCP8.5. In some parts of western Iberia, GSL values may remain largely unchanged, and this is the only area where future projections for both scenarios are non-significant (NS).

Olive yields (**Fig. 3b and 4b**), are expected to decrease mostly in the Iberian Peninsula (-30% to -45% in both scenarios) and some inner areas of Italy (down to -15%), whereas they are expected to increase in other parts of Europe (up to +15%). It should be noted that the increases in yields are comparatively small and tend to be NS. The outcomes for the two future scenarios are in agreement, though a stronger climate change signal is expected under RCP8.5 (**Fig 4b**). In order to assess the climate model uncertainty, i.e. differences between the outputs from the four climate model pairs, the point-by-point normalized interquartile ranges (NIQR) of the yield outputs from each model were computed. **Figure 5** shows that the uncertainty is relatively low over all of southern Europe, with some small regions in Iberia showing slightly higher uncertainties, mostly under RCP8.5. Hence, the climate change projections provided by the ensemble of 4 RCM-GCM model chains may be considered as robust.

Regarding GST under RCP4.5 and 8.5 (**Fig. 3c and 4c**, respectively), a clear warming of the growing season is found throughout southern Europe, intensified under the severest scenario (RCP8.5). In fact, GST is expected to increase by up to 2 or 3 ºC (for RCP4.5 and RCP8.5, respectively), leading to the increase in GSL. Larger changes are projected in inner Iberia, that shows GST increases of 2.5ºC with respect to the recent-past. Regarding future GSP (**Fig. 3d** and **4d**, for RCP4.5 and 8.5, respectively), both scenarios depict important decreases in the Iberian Peninsula, mainly under RCP8.5 (**Fig. 4d**). Conversely, increases up to 100 mm are projected in GSP over the easternmost areas (Italy, Greece and Turkey), although for some of these areas the results are NS.

ETP is expected to increase from 30 to 75 mm in RCP4.5 (**Fig. 3e**), and from 45 to 90 mm in RCP8.5 (**Fig. 4e**). These results are in accordance with Tanasijevic *et al.* (2014), who projected an olive ET increase of around 51(±17) mm up to the middle of this century under the A1B scenario. Southern Iberia is projected to have the strongest increase in this metric. Contrarily to the ETP, ETA will decrease in most of the olive orchard area during the XXI Century. Under RCP4.5 (**Fig. 3f**), these values will strongly decrease in southern Iberia (-75 mm), particularly in Portugal (-100 mm). Over southern France and northern Italy, there may be a slight NS increase in ETA, as is the case of the increased GSP. Under RCP8.5 (**Fig. 4f**), these impacts will be intensified, particularly in southern Iberia.

These projected changes (increase in ETP and decrease in ETA), higher water demands and lower water availability, will enhance water stress for olive trees in the future. Under RCP4.5 (**Fig. 3g**), WD is expected to rise by 90 to 135 mm, particularly in southern Iberia. There are some small regions where WD could decrease, especially along coastal areas in the Adriatic. Under RCP8.5 (**Fig. 4g**), these changes are strengthened. Changes in WP are spatially heterogeneous for both scenarios (**Fig. 3h and 4h**). WP tends to decrease in eastern southern Iberia and in some regions of central Italy, decreasing elsewhere.

3.3 Regional inter-annual variability in yields

Figure 6 depicts the box-plots representing simulated yields for all years and scenarios and for each of the olive producing regions in Europe (from 1989 to 2005 for the recent-past and from 2041 to 2070 for both RCPs). In terms of means and medians, all regions show lower future yields (**Table 3**), with the exceptions of Puglia and Peloponnese, which show higher yields for both future scenarios with respect to the present period. The strongest negative impacts are found in Andalucía, Alentejo and Extremadura and for RCP8.5. Both scenarios are in agreement in terms of climate change signal, while RCP8.5 provides the strongest changes in magnitude, either positive or negative (**Table 3**).

Concerning the yield extremes (99th and 1st percentiles), future projections highlight stronger variability in all regions. Regarding the interquartile ranges - IQR (75th percentile minus 25th percentile), some regions show lower future inter-annual variability, such as Alentejo, Andalucía, Extremadura and Castilla la Mancha, while others show higher future annual variability, i.e. Sardegna, Sicily, Puglia and Peloponnese (**Fig. 6**). Thus, most regions are expected to suffer negative impacts both in terms of yield losses and higher variability.

4. Discussion and conclusions

The present study focused on the application of crop models to quantify present (1989–2005) and future (2041–2070) olive growing season climatic conditions over southern Europe, including seasonal cycle length, yield, water demand and water productivity. Under recent climatic conditions, the season-model shows a latitudinal gradient, i.e. the olive tree growing season is longer/shorter at lower/higher latitudes. The yield-model shows lower yields in western European olive growing areas, especially in inner Iberia, whereas higher yields are found in the eastern areas, such as Italy and Greece. Regarding the GST, higher values are found in inner Iberia, while GSP shows similar values throughout European olive orchards, with the exception of western Italy. Regarding ETP and ETA, they show patterns very similar to GST and GSP, respectively. This also underlies higher WD in inner Iberia. Regarding WP, similar values are found throughout the orchard areas in Europe.

Although the simulated yields depict an agreement with statistical datasets and the model provides a realistic magnitude of yield values, some model bias were identified. These can be attributed to inherent differences between simulated and statistical datasets, such as the different time periods and different spatial resolution (country average data vs. grid data). Additionally, the large spatial extent of the target area required some assumptions in model parameterizations, such as regional cultural practices and varieties. These assumptions, such as setting a fixed LAI or planting density throughout European olive orchards, may increase the bias of the final outcomes, especially when considering that high density irrigated orchards have been introduced in many areas. It is important to recognize that the regional yield differences are not only dependant on regional soil and climate conditions, but also on technological advances, higher plant density and other key agricultural operations. Nonetheless, such detailed information is not currently available for the large spatial extent, needed for the model runs. In fact, the Mediterranean basin encompasses a wide range of olive tree varieties, different cultivation systems and agronomic practices (Moriondo *et al.*, 2015, Ponti *et al.*, 2014). While these factors restrict the prediction of yields over such as vast area, they allow a thorough climate change impact assessment, as they take into account only the climate change signal. Nonetheless, the different spatial gradients in European olive growing regions were skilfully modelled, such as the differences in yields between the western (lower yields) and eastern (higher yields) olive growing regions in southern Europe. Another important aspect limiting the model prediction accuracy is tied to the model development state. At the moment, perennial crop models, and consequently olive tree models, present various limitations, which restrict their accuracy and application. As an example, the models used herein do not explicitly consider the anthesis state, which might be of major interest for growers. In the future, advances in crop modelling techniques and development may surpass these limitations and thus permit wider applications.

The crop model projections indicate that olive trees will be affected by considerable challenges in the future decades. The projections point to a general increase in the length of the potential growing season (GSL), due to the increase in temperatures. As the heat accumulation is generally higher, physiological activity may occur earlier. Although the overall higher temperatures in the growing season may have positive impacts, other factors, such as extreme temperatures during the warmer part of the year, may offset this positive effect. These impacts are also intensified by the already reported advancement in olive flowering (Avolio *et al.*, 2012, Orlandi *et al.*, 2012), which may bring additional threats to the sector, such as the risk of pests and diseases (Ribeiro *et al.*, 2009). Our results also indicate GST in southern Europe combined with lower/higher GSP in the western/eastern areas, leading to a higher WD in the western olive producing regions, which will ultimately impact yields. Hence, there is a clear cause-effect relationship between the increases in GST, ETP and WD, the decreases in GSP and ETA, and the projected yield decrease for the future. Our results suggest that olive productivity in Southern Europe will probably decrease in the western areas, particularly in the Iberian Peninsula. These results are in agreement with older studies using the A1B scenario (Ponti *et al.*, 2014, Tanasijevic *et al.*, 2014). Conversely, climate change will tend to benefit some olive-producing areas particularly in the eastern parts of southern Europe. These outcomes are not in line with Tanasijevic *et al.* (2014), who suggests a decrease in suitability future rainfed olive cultivation in Italy and Greece. It should be noted that the mentioned study uses an older IPCC scenario and older model simulations (previous assessment report) and the current study uses an ensemble of state-of-the-art climate models and two future RCPs.

Herein we show for the first time future impacts on European olive productivity based on an ensemble of state-of-the-art climate models, future scenarios and crop models. Given the results shown in the current study, climate change may negatively impact the viability of farms in southern Iberia and, consequently, increase the risk of abandonment of olive groves (de Graaff *et al.*, 2010). To cope with the projected changes, an adequate and timely planning of suitable adaptation measures needs to be adopted by the olive sector, particularly in Iberia.

One of the main adaptation measures to future drier climates in these areas is the improvement of water use efficiency. Water scarcity and competition will be one of the main problems in these areas in the future, and smart irrigation strategies should be planned and implemented (Gomez-Rico *et al.*, 2007, Orlandi *et al.*, 2012, Tanasijevic *et al.*, 2014). These practices are already being adopted, accompanied by the implementation of intensive plantation systems instead of traditional olive groves. As an example, smart irrigation systems are already being installed in many groves in southern Spain (Tanasijevic *et al.*, 2014). This indicates a growing concern about the future sustainability of the sector, as well as an increasing awareness of the potential threats. However, sufficient water supply should be taken into account, as in these areas this important resource is scarce, particularly due to the prolonged low water availability periods during summer and to strong water competition, by other crops (e.g. horticulture), by hydropower generation and by human consumption (e.g. domestic use and tourism). An additional/complementary adaptation measure to irrigation would be to increase WP, by selecting more adapted olive tree varieties, with higher drought and heat tolerance, thus requiring less water to obtain similar yield levels. Regarding WD, it should be mentioned that olive trees adapt exceptionally well to the typically dry conditions of Mediterranean-type climates, e.g. by capturing water from soils under the wilting point, which may result in actual lower WD.

Other adaptation measures should also be envisioned, which may provide additional positive gains under climate chance. Moreover, the implications of using intensive vs. traditional systems should be studied (Patumi *et al.*, 1999). Longer-term measures should also be anticipated, such as the northward shift of olive tree cultivation and/or its displacement to higher elevations in order to avoid areas with severe/extreme heat stress (Orlandi *et al.*, 2012). One potentially beneficial aspect of climate change that should be considered is the increase in CO_2 levels. Some studies have shown that increased CO_2 concentration may bring positive physiological effects, namely on photosynthesis (Drake *et al.*, 1997). In fact, the yield-model considers this effect in the photosynthesis sub-model, which takes into account the CO_2 concentration. Hence, the present study considers this effect to a certain extent, as higher CO_2 may mitigate some of the negative effects of climate change, particularly droughts.

The adoption of suitable adaptation measures should be explored in each olive orchard, taking into account theirs specificities, as they might be required to warrant the future sustainability of the olive sector. In fact, the sector's ability to adapt to climate change will determine the magnitude of the projected impacts (Quiroga & Iglesias, 2009). The current study is a first approach using these crop models at such a large-scale level (Europe). It is thereby necessary to continue evaluating and improving these tools so as to attain more accurate information regarding climate change impacts on olive trees, as well as to develop effective and sustainable adaptation measures to cope with climate change.

Acknowledgements

This work was funded by European Investment Funds (FEDER/COMPETE/POCI), POCI-01-0145-FEDER-006958, and by the Portuguese Foundation for Science and Technology (FCT), UID/AGR/04033/2013. The postdoctoral fellowship (SFRH/BPD/119461/2016) awarded to the first author is appreciated. This work was partially funded by the FCT contract CEECIND/00447/2017. JGP thanks the AXA Research Fund for support.

Declaration on conflict of interest

The authors declare no conflict of interest.

References

Aguilera F, Dhiab AB, Msallem M *et al.* (2015) Airborne-pollen maps for olive-growing areas throughout the Mediterranean region: spatio-temporal interpretation. Aerobiologia, 31, 421-434, https://doi.org/10.1007/s10453-015-9375-5.

Aissaoui F, Chehab H, Bader B *et al.* (2016) Early water stress detection on olive trees (Olea europaea L. cvs 'chemlali' and 'Chetoui') using the leaf patch clamp pressure probe. Computers and Electronics in Agriculture, 131, 20-28, https://doi.org/10.1016/j.compag.2016.11.007.

Avolio E, Orlandi F, Bellecci C, Fornaciari M, Federico S (2012) Assessment of the impact of climate change on the olive flowering in Calabria (southern Italy). Theoretical and Applied Climatology, 107, 531-540, https://doi.org/10.1007/s00704-011-0500-2.

Cesaraccio C, Spano D, Snyder RL, Duce P (2004) Chilling and forcing model to predict bud-burst of crop and forest species. Agricultural and Forest Meteorology, 126, 1-13, https://doi.org/10.1016/j.agrformet.2004.03.002.

Challinor AJ, Wheeler TR (2008) Crop yield reduction in the tropics under climate change: Processes and uncertainties. Agricultural and Forest Meteorology, 148, 343-356, https://doi.org/10.1016/j.agrformet.2007.09.015.

Cofiño AS, Bedia J, Iturbide M *et al.* (2017) The ECOMS User Data Gateway: Towards seasonal forecast data provision and research reproducibility in the era of Climate Services. Climate Services, https://doi.org/10.1016/j.cliser.2017.07.001.

De Graaff J, Duarte F, Fleskens L, De Figueiredo T (2010) The future of olive groves on sloping land and ex-ante assessment of cross compliance for erosion control. Land Use Policy, 27, 33-41, https://doi.org/10.1016/j.landusepol.2008.02.006.

De Melo-Abreu JP, Barranco D, Cordeiro AM, Tous J, Rogado BM, Villalobos FJ (2004) Modelling olive flowering date using chilling for dormancy release and thermal time. Agricultural and Forest Meteorology, 125, 117-127, https://doi.org/10.1016/j.agrformet.2004.02.009.

Dee DP, Uppala SM, Simmons AJ *et al.* (2011) The ERA-Interim reanalysis: configuration and performance of the data assimilation system. Quarterly Journal of the Royal Meteorological Society, 137, 553-597, https://doi.org/10.1002/qj.828.

Deser C, Phillips A, Bourdette V, Teng HY (2012) Uncertainty in climate change projections: the role of internal variability. Climate Dynamics, 38, 527-546, https://doi.org/10.1007/s00382-010-0977-x.

Drake BG, Gonzalezmeler MA, Long SP (1997) More efficient plants: A consequence of rising atmospheric CO2? Annual Review of Plant Physiology and Plant Molecular Biology, 48, 609-639.

Ec (2012) Economic analysis of the olive sector. pp 10.

Fao/Iiasa/Isric/Isscas/Jrc (2012) Harmonized World Soil Database (version 1.2). FAO, Rome, Italy and IIASA, Laxenburg, Austria.

Fraga H, Pinto JG, Santos JA (2019) Climate change projections for chilling and heat forcing conditions in European vineyards and olive orchards: a multi-model assessment. Climatic Change, 152, 179-193, https://doi.org/10.1007/s10584-018-2337-5.

Galán C, García-Mozo H, Vázquez L, Ruiz L, De La Guardia CD, Trigo MM (2005) Heat requirement for the onset of the Olea europaea L. pollen season in several sites in Andalusia and the effect of the expected future climate change. International Journal of Biometeorology, 49, 184-188, https://doi.org/10.1007/s00484-004-0223-5.

Garcia-Mozo H, Orlandi F, Galan C *et al.* (2008) Olive flowering phenology variation between different cultivars in Spain and Italy: modeling analysis. Theoretical and Applied Climatology, 95, 385, https://doi.org/10.1007/s00704-008-0016-6.

Giorgi F (2006) Climate change hot-spots. Geophysical Research Letters, 33, https://doi.org/10.1029/2006gl025734.

Gomez-Rico A, Salvador MD, Moriana A, Perez D, Olmedilla N, Ribas F, Fregapane G (2007) Influence of different irrigation strategies in a traditional Cornicabra cv. olive orchard on virgin olive oil composition and quality. Food Chemistry, 100, 568-578, https://doi.org/10.1016/j.foodchem.2005.09.075.

Ioc (2018) International Olive Council statistical series. http://www.internationaloliveoil.org.

Ipcc (2012) Managing the Risks of Extreme Events and Disasters to Advance Climate Change Adaptation. A Special Report of Working Groups I and II of the Intergovernmental Panel on Climate Change [Field, C.B., V. Barros, T.F. Stocker, D. Qin, D.J. Dokken, K.L. Ebi, M.D. Mastrandrea, K.J. Mach, G.-K. Plattner, S.K. Allen, M. Tignor, and P.M. Midgley (eds.)]. Cambridge University Press, Cambridge, UK, and New York, NY, USA, 582 pp.

Jacob D, Petersen J, Eggert B *et al.* (2014) EURO-CORDEX: new high-resolution climate change projections for European impact research. Regional Environmental Change, 14, 563-578, https://doi.org/10.1007/s10113-013-0499-2.

Maselli F, Chiesi M, Brilli L, Moriondo M (2012) Simulation of olive fruit yield in Tuscany through the integration of remote sensing and ground data. Ecological Modelling, 244, 1-12, https://doi.org/10.1016/j.ecolmodel.2012.06.028.

Moriondo M, Ferrise R, Trombi G, Brilli L, Dibari C, Bindi M (2015) Modelling olive trees and grapevines in a changing climate. Environmental Modelling & Software, 72, 387-401, https://doi.org/10.1016/j.envsoft.2014.12.016.

Moriondo M, Leolini L, Brilli L *et al.* (2019) A simple model simulating development and growth of an olive grove. European Journal of Agronomy, 105, 129-145, https://doi.org/10.1016/j.eja.2019.02.002.

Moriondo M, Orlandini S, Nuntiis PD, Mandrioli P (2001) Effect of agrometeorological parameters on the phenology of pollen emission and production of olive trees (Olea europea L.). Aerobiologia, 17, 225-232, https://doi.org/10.1023/A:1011893411266.

Moriondo M, Trombi G, Ferrise R *et al.* (2013) Olive trees as bio-indicators of climate evolution in the Mediterranean Basin. Global Ecology and Biogeography, 22, 818-833, https://doi.org/10.1111/geb.12061.

Orlandi F, Avolio E, Bonofiglio T, Federico S, Romano B, Fornaciari M (2012) Potential shifts in olive flowering according to climate variations in Southern Italy. Meteorological Applications, 20, 497-503, https://doi.org/10.1002/met.1318.

Orlandi F, Garcia-Mozo H, Dhiab AB *et al.* (2013) Climatic indices in the interpretation of the phenological phases of the olive in mediterranean areas during its biological cycle. Climatic Change, 116, 263-284, https://doi.org/10.1007/s10584-012-0474-9.

Orlandi F, Garcia-Mozo H, Galán C *et al.* (2010) Olive flowering trends in a large Mediterranean area (Italy and Spain). International Journal of Biometeorology, 54, 151-163, https://doi.org/10.1007/s00484-009-0264-x.

Orlandi F, Ruga L, Romano B, Fornaciari M (2005) Olive flowering as an indicator of local climatic changes. Theoretical and Applied Climatology, 81, 169-176, https://doi.org/10.1007/s00704-004-0120-1.

Osborne CP, Chuine I, Viner D, Woodward FI (2000) Olive phenology as a sensitive indicator of future climatic warming in the Mediterranean. Plant Cell and Environment, 23, 701-710, https://doi.org/10.1046/j.1365-3040.2000.00584.x.

Osborne CP, Chuine I, Viner D, Woodward FI (2001) Olive phenology as a sensitive indicator of future climatic warming in the Mediterranean. Plant, Cell & Environment, 23, 701-710, https://doi.org/10.1046/j.1365-3040.2000.00584.x.

Oteros J, Orlandi F, García-Mozo H *et al.* (2014) Better prediction of Mediterranean olive production using pollen-based models. Agronomy for Sustainable Development, 34, 685-694, https://doi.org/10.1007/s13593-013-0198-x.

Patumi M, D'andria R, Fontanazza G, Morelli G, Giorio P, Sorrentino G (1999) Yield and oil quality of intensively trained trees of three cultivars of olive (Olea europaea L.) under different irrigation regimes. Journal of Horticultural Science & Biotechnology, 74, 729-737.

Paz JO, Fraisse CW, Hatch LU *et al.* (2007) Development of an ENSO-based irrigation decision support tool for peanut production in the southeastern US. Computers and Electronics in Agriculture, 55, 28-35, https://doi.org/10.1016/j.compag.2006.11.003.

Perry C (2011) Accounting for water use: Terminology and implications for saving water and increasing production. Agricultural Water Management, 98, 1840-1846, https://doi.org/10.1016/j.agwat.2010.10.002.

Ponti L, Gutierrez AP, Ruti PM, Dell'aquila A (2014) Fine-scale ecological and economic assessment of climate change on olive in the Mediterranean Basin reveals winners and losers. Proceedings of the National Academy of Sciences of the United States of America, 111, 5598-5603, https://doi.org/10.1073/pnas.1314437111.

Quiroga S, Iglesias A (2009) A comparison of the climate risks of cereal, citrus, grapevine and olive production in Spain. Agricultural Systems, 101, 91-100, https://doi.org/10.1016/j.agsy.2009.03.006.

Ribeiro H, Cunha M, Abreu I (2009) A bioclimatic model for forecasting olive yield. Journal of Agricultural Science, 147, 647-656, https://doi.org/10.1017/s0021859609990256.

Saxton KE, Rawls WJ, Romberger JS, Papendick RI (1986) Estimating Generalized Soil-water Characteristics from Texture. Soil Science Society of America Journal, 50, 1031-1036, https://doi.org/10.2136/sssaj1986.03615995005000040039x.

Semenov MA, Doblas-Reyes FJ (2007) Utility of dynamical seasonal forecasts in predicting crop yield. Climate Research, 34, 71-81, https://doi.org/10.3354/Cr034071.

Tanasijevic L, Todorovic M, Pereira LS, Pizzigalli C, Lionello P (2014) Impacts of climate change on olive crop evapotranspiration and irrigation requirements in the Mediterranean region. Agricultural Water Management, 144, 54-68, https://doi.org/10.1016/j.agwat.2014.05.019.

Villalobos FJ, Orgaz F, Testi L, Fereres E (2000) Measurement and modeling of evapotranspiration of olive (Olea europaea L.) orchards. European Journal of Agronomy, 13, 155-163, https://doi.org/10.1016/S1161-0301(00)00071-X.

Villaobos FJ, Testi L, Hidalgo J, Pastor M, Orgaz F (2006) Modelling potential growth and yield of olive (Olea europaea L.) canopies. European Journal of Agronomy, 24, 296-303, https://doi.org/10.1016/j.eja.2005.10.008.

Viola F, Noto LV, Cannarozzo M, La Loggia G, Porporato A (2012) Olive yield as a function of soil moisture dynamics. Ecohydrology, 5, 99-107, https://doi.org/10.1002/eco.208.

Vossen P (2007) Olive oil: History, production, and characteristics of the world's classic oils. HortScience, 42, 1093-1100.

Table 1 – List of the regional climate models (RCM) and used boundary conditions from global climate models (GCM) used in this study.

RCM	**GCM**
CLMcom-CCLM4-8-17	MPI-M-MPI-ESM-LR
IPSL-INERIS-WRF331F	IPSL-IPSL-CM5A-MR
KNMI-RACMO22E	ICHEC-EC-EARTH
SMHI-RCA4	CNRM-CERFACS-CNRM-CM5

Table 2 - Soil and terrain parameters used in the crop model, along with the corresponding datasets used for their calculation and key references.

Parameter	Calculation
Clay content (%)	HWSD
Sand content (%)	HWSD
Silt content (%)	HWSD
Field capacity fraction ($cm^3.cm^{-3}$)	Estimated following Saxton *et al.* (1986)
Soil porosity ($cm^3.cm^{-3}$)	Estimated following Saxton *et al.* (1986)
hydraulic conductivity ($cm.day^{-1}$)	Estimated following Saxton *et al.* (1986)

Table 3 – Regional mean differences, in percentage, between future (2041–2070) RCP4.5/8.5 and the present annual mean yields.

#	Region	RCP4.5	RCP8.5
1	Alentejo-PT	-17	-20
2	Andalucía-ES	-17	-21
3	Extremadura-ES	-15	-19
4	Castilla la Mancha-ES	-18	-19
5	Sardegna-IT	-8	-3
6	Sicily-IT	0	-8
7	Puglia-IT	5	7
8	Peloponnese-GR	4	3

Figures

Fig. 1 – Olive orchard distribution in Europe following the CORINE land cover dataset. The different color represent country yields according to FAO statistics. Additionally some of Europe top olive producing regions are also represented following NUTS 2 level delimitations.

Fig. 2 – Patterns for the recent-past (1989-2005) for *a)* Growing season length (days), *b)* yield (kg.ha^{-1}), *c)* growing season mean temperature (ºC), *d)* Growing season precipitation sum (mm), *e)* potential evapotranspiration in the growing season (mm), *f)* actual evapotranspiration in the growing season (mm), *g)* water deficit (ETP minus ETA; mm) in the growing season, *h)* Water productivity (kg.ha^{-1}.mm; yield divided by ETA) in the growing season.

Fig. 3 – Patterns for the differences between future RCP4.5 (2041-2070) and recent-past (1989-2005) for the same variables as in Figure 2. Statistically significant (*p*-value < 0.01) and non-significant differences are also plotted in grey shading.

Fig. 4 – Same as Figure 3 but for RCP8.5.

Fig. 5 – Model uncertainty represented by the yield normalized interquartile range of the 4 RCM-GCM model chains under a) RCP4.5 and b) RCP8.5.

Fig. 6 – Box-plots representing the inter-annual variability in yields in the main Olive producing regions in Europe, for the present (1989-2005), RCP4.5 (2041-2070) and RCP8.5 (2041-2070).

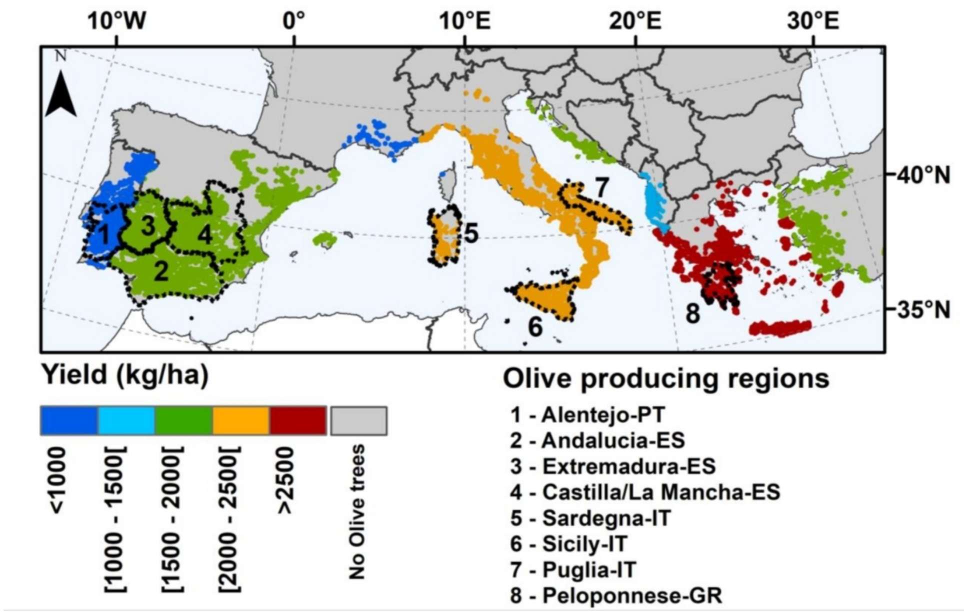

Figure 1: Olive orchard distribution in Europe following the CORINE land cover dataset. The different color represent country yields according to FAO statistics. Additionally some of Europe top olive producing regions are also represented following NUTS 2 level delimitations.

169x115mm (300 x 300 DPI)

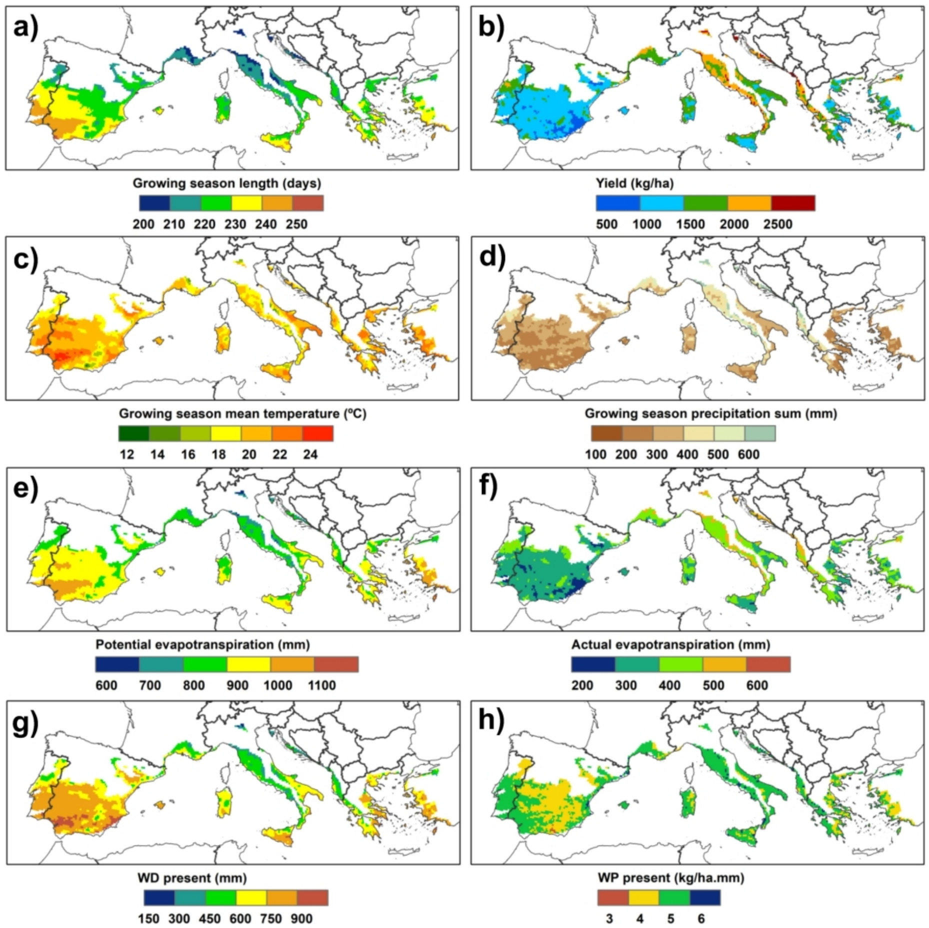

Figure 2: Patterns for the recent-past (1989-2005) for a) Growing season length (days), b) Potential yield (kg.ha-1), c) growing season mean temperature (ºC), d) Growing season precipitation sum (mm), e) potential evapotranspiration in the growing season (mm), f) actual evapotranspiration in the growing season (mm), g) water deficit (ETP minus ETA; mm) in the growing season, h) Water productivity (kg.ha-1.mm; yield divided by ETA) in the growing season.

190x187mm (300 x 300 DPI)

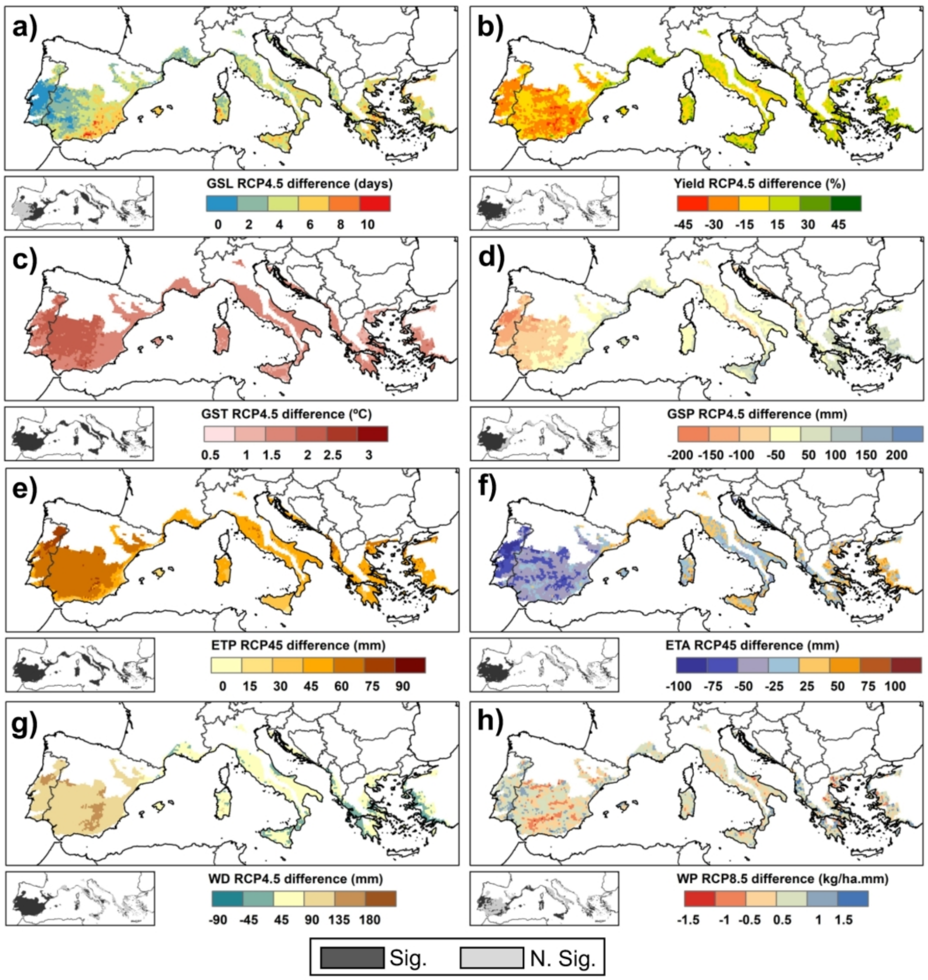

Figure 3: Patterns for the differences between future RCP4.5 (2041-2070) and recent-past (1989-2005) for the same variables as in Figure 2. Statistically significant (p-value < 0.01) and non-significant differences are also plotted in grey shading.

190x199mm (300 x 300 DPI)

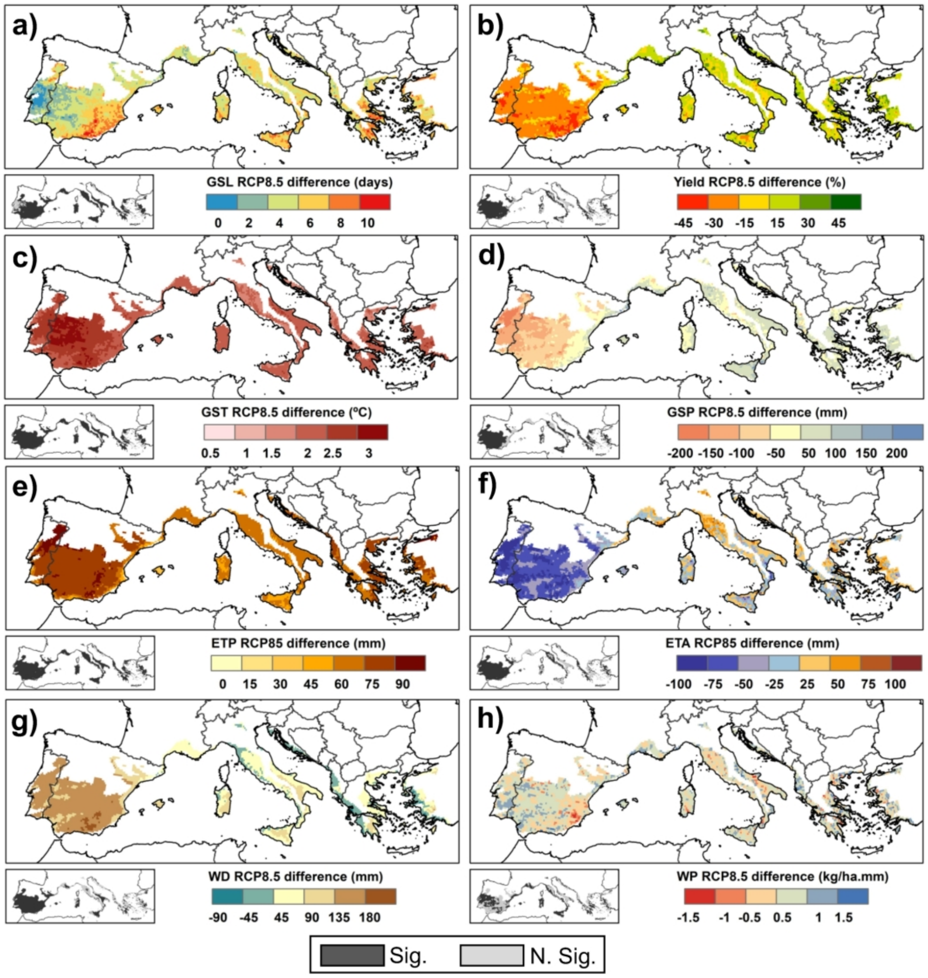

Figure 4: Same as Figure 3 but for RCP8.5.

190x197mm (300 x 300 DPI)

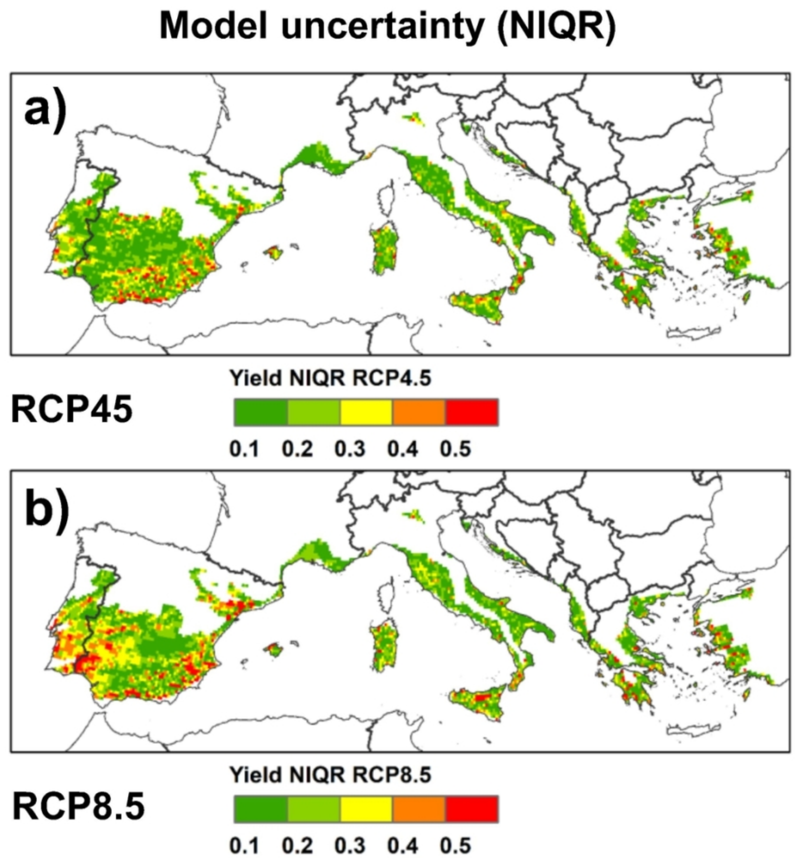

Figure 5: Model uncertainty represented by the yield normalized interquartile range of the 4 RCM-GCM model chains under a) RCP4.5 and b) RCP8.5.

110x103mm (300 x 300 DPI)

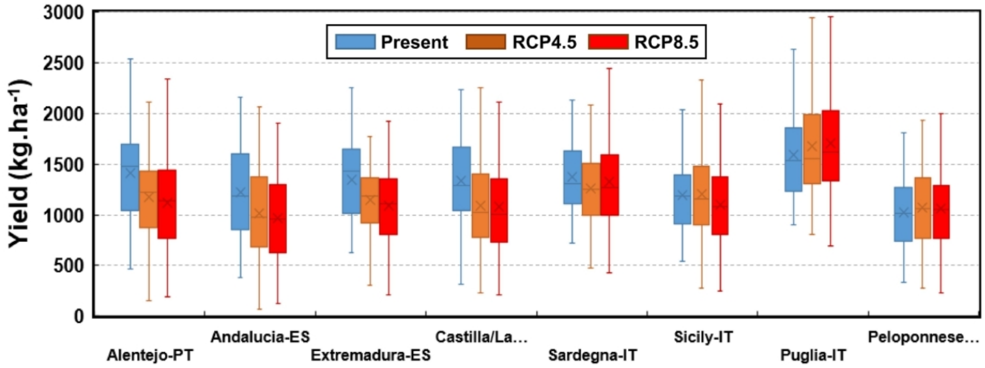

Figure 6: Box-plots representing the inter-annual variability in yields in the main Olive producing regions in Europe, for the present (1989-2005), RCP4.5 (2041-2070) and RCP8.5 (2041-2070).

190x73mm (300 x 300 DPI)

Climate change projections for olive yields in the Mediterranean Basin

Helder Fraga*; Joaquim G. Pinto; Francesco Viola; João A. Santos

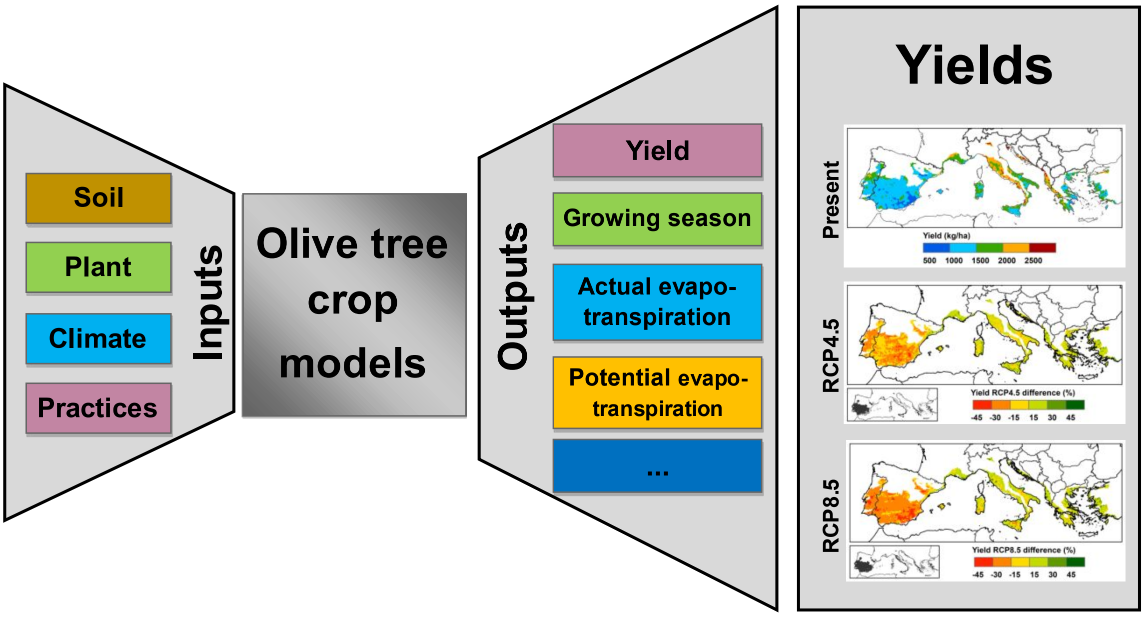

Caption: Representation of the dynamical crop models used in the present study, along with the main inputs and outputs. Yield outputs of the recent-past and future (RCP4.5 and 8.5, mean of 4 RCM-RCM model-chain ensemble) are also shown. In some parts of Eastern Europe, future yields are projected to increase by 15%. Conversely, in the warmest and driest areas of Iberia, future yields may decrease to -45%. Adaptation measures should be adopted to counteract these negative impacts under climate change scenarios.